MORPHOLOGIES AND ENZYMATIC DEGRADABILITY OF MELT-CRYSTALLIZED POLY(3-HYDROXYBUTYRIC ACID-*CO*-6-HYDROXYHEXANOIC ACID)

Hideki Abe, Hiromichi Aoki, and Yoshiharu Doi*

Polymer Chemistry Laboratory, The Institute of Physical and Chemical Research (RIKEN), Hirosawa, Wako-shi, Saitama 351-01, Japan

Abstract: The films of poly[(*R*)-3-hydroxybutyric acid-*co*-10mol% 6-hydroxyhexanoic acid] (P[(*R*)-3HB-*co*-6HH]) were prepared by melt-crystallized method at various crystallization temperatures. The morphologies and properties of melt-crystallized films were characterized by means of x-ray diffraction, differential scanning calorimetry, optical microscopy, and scanning electron microscopy. All of the melt-crystallized films showed the banded spherulite morphology. The enzymatic degradation of melt-crystallized films was carried out at 37 °C in an aqueous solution (pH 7.4) of PHB depolymerase from *Alcaligenes faecalis*. The rate of enzymatic erosion was strongly dependent on the crystallinity of films, and the highest rate was as large as 2.15 $mg \cdot h^{-1} \cdot cm^{-2}$. After enzymatic degradation, the banded morphology of P[(*R*)-3HB-*co*-6HH] spherulites was visible, suggesting that PHB depolymerase predominantly hydrolyzes polymer chains on the edges of crystalline lamellar stacks.

INTRODUCTION

The microbial poly(hydroxyalkanoic acids) (PHA) family of polyesters is biodegradable thermoplastic produced from various carbon substrates by a number of bacteria (Ref. 1). The PHA has been shown to be formed as a storage material in over 90 genera of bacteria, and 91 different constituents of PHA have been identified as various hydroxyalkanoic acids with three to fourteen carbon atoms (Ref. 2). These biodegradable PHA polymers have attracted much attention as environmentally degradable thermoplastics to be used for a wide range of agricultural, marine, and medical applications. A remarkable characteristic of PHA is their biodegradability in various environments (Refs. 3,4). A number of microorganisms such as bacteria and fungi in environments excrete PHB depolymerases to hydrolyze the solid PHA into water-soluble oligomers and monomer, and they utilize the resulting products as nutrients within cells. Aerobic and anaerobic PHA-degrading microorganisms have been isolated from various ecosystems, and the properties of their extracellular PHB depolymerases have been studied (Refs. 5–7).

 CCC 1022-1360/98/$ 10.00

In a previous paper (Ref. 8), we prepared novel copolymers of (*R*)-3-hydroxybutyric acid ((*R*)-3HB) and 6-hydroxyhexanoic acid (6HH) with a wide range of compositions by the ring-opening polymerization of (*R*)-β-butyrolactone with ε-caprolactone in the presence of distannoxane as a catalyst, and studied the enzymatic degradation of the solvent-cast films in the presence of PHB depolymerase from *Alcaligenes faecalis* or of lipase from *Rhizopus delemar*. The highest rate of enzymatic hydrolysis by PHB depolymerase was observed at 10 mol% 6HH, while the highest rate of enzymatic hydrolysis by lipase was observed at 90 mol% 6HH. In this paper, we report the morphologies and enzymatic degradability for melt-crystallized films of a random copolymer of 90 mol% (*R*)-3HB and 10 mol% 6HH units.

EXPERIMENTAL

All films were initially prepared by conventional solvent-cast techniques from chloroform solutions of P[(*R*)-3HB-*co*-6HH] using glass Petri dishes as casting surfaces. Solvent-cast films were inserted between two Teflon sheets with a Teflon sheet (0.05 mm thickness) as a spacer and were compression-molded on a Mini Test Press (Toyoseiki) by heating at 200 °C for 1 min under a pressure of 75 $kg \cdot cm^{-2}$. After melting, samples were kept at a given crystallization temperature (Tc) and isothermally crystallized for 3 days.

The extracellular PHB depolymerase was purified to electrophoretic homogeniety from *A. faecalis*. The enzymatic degradation of melt-crystallized P[(*R*)-3HB-*co*-6HH] films was carried out at 37 °C in 0.1 M potassium phosphate buffer (pH 7.4). Films (initial weights, about 6 mg; initial dimensions, 10×10×0.05 mm) were placed in small glass bottles containing 1.0 ml of phophate buffer. The reaction was started by the addition of 2.6 μl of an aqueous solution of PHB depolymerase (1.0 μg). The reaction solution was incubated at 37±0.1 °C with shaking, and the sample films were removed after reaction, washed with distilled water, and dried to constant weight in vacuo before analysis.

Differential scanning calorimetry (d.s.c.) data of P[(*R*)-3HB-*co*-6HH] samples were recorded in the temperature range 0 to 200 °C on a Shimadzu DSC-50 equipped with a cooling accessory under a nitrogen flow of 30 $ml \cdot min^{-1}$. Samples of 10 mg were encapsulated in aluminum pans and heated from 0 to 200 °C at a rate of 20 $°C \cdot min^{-1}$. The melting temperature (Tm) and enthalpy of fusion (ΔHm) were determined from the d.s.c. endotherms. The Tm was taken as the peak temperature.

The x-ray diffraction patterns of films were recorded at 27 °C on a Rigaku RAD-IIIB system using nickel-filtered Cu Kα radiation (λ=0.154 nm; 40 kV; 30 mA) in the 2θ range 6–60 ° at a scan speed of 3.0 $° \cdot min^{-1}$. Degrees of crystallinity (Xc) of P[(*R*)-3HB-*co*-6HH] films were calculated from diffracted intensity data according to Vonk's method (Ref. 8).

The surface appearances of films were obtained with a scanning electron microscope (JEOL JSM-T220) after gold coating of melt-crystallized P[(*R*)-3HB-*co*-6HH] films using an ion coater. Morphologies of melt-crystallized P[(*R*)-3HB-*co*-6HH] films were observed with an optical microscope (Nikon OPTIPHOTO-2) equipped with a phase contrast lens.

RESULTS AND DISCUSSION

Poly[(*R*)-3-hydroxybutyric acid-*co*-10mol% 6-hydroxyhexanoic acid] (P[(*R*)-3HB-*co*-6HH]) was prepared by the ring-opening copolymerization of a mixture of (*R*)-β-butyrolactone and ε-caprolactone in the presence of distannoxane catalyst (Ref. 8). Number-average molecular weight (*M*n), polydispersity(*M*w/*M*n), and glass-transition temperature (Tg) of copolymer were *M*n=107,000, *M*w/*M*n=1.7, and Tg=–5 °C, respectively. From the ^{13}C nuclear magnetic resonance (n.m.r.) analysis, the sequence distribution of (*R*)-3HB and 6HH units in the copolymer was statistically random (Ref. 8). Melt-crystallized P[(*R*)-3HB-*co*-6HH] films were prepared by isothermal crystallization at different temperatures of 30–110 °C for 3 days from melt at 200 °C for 1 min. Tab. 1 lists the crystallization temperature, thermal properties, and degree of crystallinity for the melt-crystallized P[(*R*)-3HB-*co*-6HH] films. All P[(*R*)-3HB-*co*-6HH] films showed the well-developed and volume-filled spherulites. Fig. 1 shows the typical optical micrographs of P[(*R*)-3HB-*co*-6HH] spherulites grown at a given temperature. The mean spherulite size increased with increasing crystallization temperature due to a decrease in the nucleation rate. In addition, the spherulites of P[(*R*)-3HB-*co*-6HH] films showed the banded morphology owing to the difference in orientation of crystalline lamellae. Fig. 2 shows the band spacing of P[(*R*)-3HB-*co*-6HH] spherulites grown at different crystallization temperatures. The band spacing of spherulites increased from around 7 μm to 17 μm with increasing the crystallization temperature from 70 °C to 100 °C.

The crystalline structure of melt-crystallized P[(*R*)-3HB-*co*-6HH] films were characterized by the x-ray diffraction analysis. The diffraction patterns of all melt-crystallized samples showed reflections arising from the crystalline lattice of poly[(*R*)-3-hydroxybutyric acid] (P[(*R*)-3HB]). The x-ray crystallinities of P[(*R*)-3HB-*co*-6HH] films were calculated from the diffraction patterns, and the data are listed in Tab. 1. The crystallinity of P[(*R*)-3HB-*co*-6HH] films ranged from 34 to 50 %, and tended to increase with crystallization temperature.

The thermal properties of melt-crystallized P[(*R*)-3HB-*co*-6HH] films were characterized by differential scanning calorimetry (d.s.c.). Fig. 3 shows a typical d.s.c. curve of P[(*R*)-3HB-*co*-6HH] film (sample 8) recorded at a heating rate of 20 °C·min^{-1}. Two endothermic peaks (Tm1 and Tm2) were detected in the thermograms of P[(*R*)-3HB-*co*-6HH] samples. In order to examine whether the peak (Tm2) at high temperature arises from a recrystallization process, the d.s.c. curves of melt-crystallized films were recorded at different heating rates of 5–40 °C·min^{-1}. As the heating rate was increased, the higher temperature peak (Tm2) became smaller while the lower temperature peak (Tm1) remained almost unaltered. The result indicates that the higher melting endothermic peak is caused by the rearrangement of an initial crystal morphology of P[(*R*)-3HB-*co*-6HH]. The lower melting temperature (Tm1) represents the melting of original crystals formed at a crystallization temperature, and the value increased with crystallization temperature, suggesting that the thickness of crystalline lamellae in melt-crystallized P[(*R*)-3HB-*co*-6HH] film increases with an increase in the crystallization temperature.

Tab. 1. Properties and rates of enzymatic erosion for melt-crystallized films of poly[(*R*)-3-hydroxybutyric acid-*co*-10mol% 6-hydroxyhexanoic acid]

Sample no.	Crystallization temperature, Tc (°C)	Melting temperature [a] (°C)		Heat of fusion [b] ($J \cdot g^{-1}$)		X-ray crystallinity, Xc (%)	Rate of enzymatic erosion ($mg \cdot h^{-1} \cdot cm^{-2}$)
		Tm1	Tm2	ΔHm1	ΔHm2		
1	30	102	130	53	49	34 ± 3	2.15 ± 0.12
2	40	106	131	56	54	43 ± 3	1.31 ± 0.08
3	50	110	131	57	50	40 ± 4	0.84 ± 0.05
4	60	112	131	60	52	43 ± 4	0.79 ± 0.07
5	65	115	131	50	47	47 ± 3	0.57 ± 0.05
6	70	116	131	69	48	50 ± 4	0.58 ± 0.06
7	75	120	132	55	47	48 ± 4	0.42 ± 0.05
8	80	119	133	64	52	43 ± 5	0.40 ± 0.04
9	85	122	133	70	50	48 ± 5	0.52 ± 0.04
10	90	124	134	56	45	45 ± 4	0.41 ± 0.05
11	95	126	134	57	46	44 ± 4	0.49 ± 0.04
12	100	128		69	44	44 ± 4	0.58 ± 0.06
13	105	129		62	39	44 ± 5	0.49 ± 0.05
14	110	130		60	34	47 ± 5	0.41 ± 0.04

a) Peak temperatures of the lower melting endotherm (Tm1) and higher melting endotherm (Tm2) on d.s.c. thermograms.

b) Enthalpies of fusion determined from d.s.c. curves. ΔHm1: onset of melting (Tm4 in Fig. 3) was adopted at room temperature, ΔHm2: onset of melting (Tm3 in Fig. 3) was adopted at about 10–15 °C above the crystallization temperature.

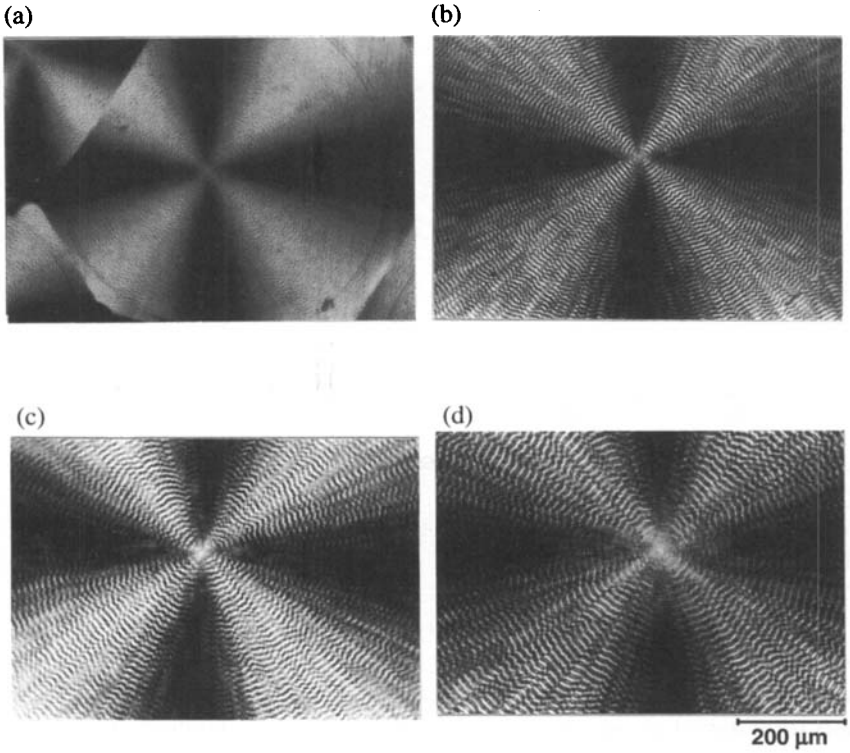

Fig. 1. Optical micrographs of melt-crystallizaed P[(*R*)-3HB-*co*-6HH] films crystallized at (a) Tc=70 °C, (b) Tc=80 °C, (c) Tc=90 °C, and (d) Tc=100 °C.

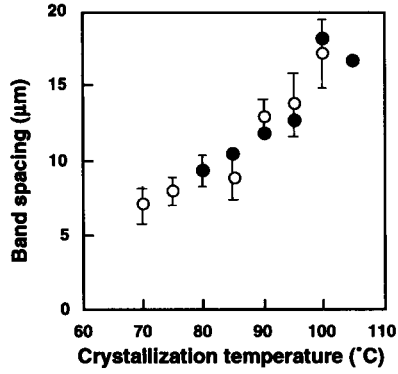

Fig. 2. Band spacing of P[(*R*)-3HB-*co*-6HH] spherulites crystallized at different temperatures. (O): the values determined from optical micrographs of sample films, (●): the values determined from scanning electron micrographs of enzymatically eroded films.

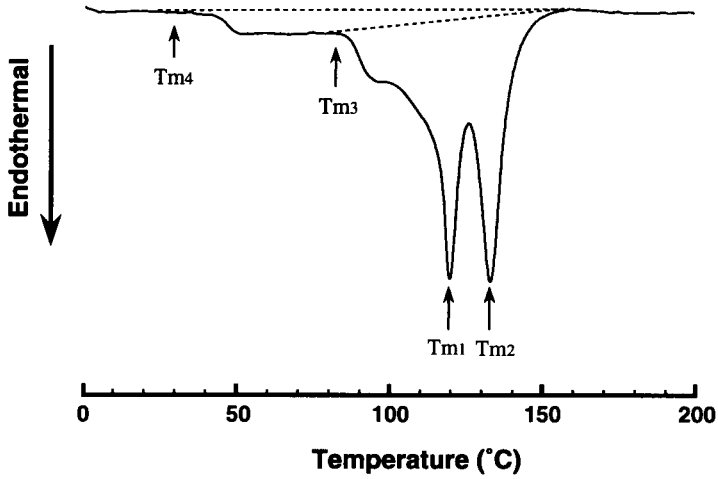

Fig. 3. Typical d.s.c. thermograms recorded at a heating rate of 20 °C·min^{-1} for P[(*R*)-3HB-*co*-6HH] film crystallized at 80 °C (sample 8).

The enthalpies of fusion for melt-crystallized P[(*R*)-3HB-*co*-6HH] films were determined from the d.s.c. curves, and the data are listed in Tab. 1. As shown in Fig.3, the melting endotherm apparently started from two different temperatures of Tm4 and Tm3. A high onset temperature (Tm3) of melting was observed at temperature of 10–15 °C above a crystallization temperature. Then, the enthalpy of fusion (ΔHm2) was determined from the onset of melting at Tm3, and the value decreased with crystallization temperature (see Tab. 1). On the other hand, the x-ray crystallinity of film increased with crystallization temperature, as shown in Tab. 1. It is of importance to note that overall melting endotherm has started from room temperature (Tm4) in the d.s.c. curve of Fig. 3. Overall enthalpy of fusion (ΔHm1) from the onset of melting at Tm4 increased with crystallization temperature, and the relative crystallinity of film calculated from the ΔHm1 value was in good agreement with the value of x-ray crystallinity of films. During the primary crystallization process at a given crystallization temperature, relatively long sequences of (*R*)-3HB units in a random copolyester may be crystallized in P[(*R*)-3HB] crystalline lamellae, while shorter sequences may remain in amorphous region, resulting in the formation of relatively thick crystalline lamellae. In this study, melt-crystallized films were allowed to stand at room temperature before analytical measurements. Then, relatively thin crystalline lamellae may be formed from shorter sequences of (*R*)-3HB units during the following crystallization process at room temperature. As a result, the melting endotherm may start from two different temperatures of Tm4 and Tm3.

The enzymatic hydrolysis of melt-crystallized P[(*R*)-3HB-*co*-6HH] films was carried out in 0.1 M potassium phosphate buffer (pH 7.4) containing PHB depolymerase (1.0 μg·ml^{-1})

from *Alcaligenes faecalis* at 37 °C. Typical weight loss profiles of P[(*R*)-3HB-*co*-6HH] films during the enzymatic hydrolysis are shown in Fig. 4. The weight loss of film increased proportionally with time. The rate of enzymatic erosion was determined from the slope of line in Fig. 4, and the data are listed in Tab. 1. The rate of enzymatic erosion decreased as the crystallization temperature of film was increased. It has been reported that PHB depolymerase initially hydrolyzes amorphous P[(*R*)-3HB] chains on the surface and subsequently erodes the polymer chains in the crystalline state (Refs. 9–11). In addition, the rate of enzymatic hydrolysis for polyester chains in amorphous region has been found to be much faster than that in crystalline region (Ref. 11). Then, a decrease in the enzymatic erosion rate of melt-crystallized P[(*R*)-3HB-*co*-6HH] film with crystallization temperature may be caused by an increase in the crystallinity.

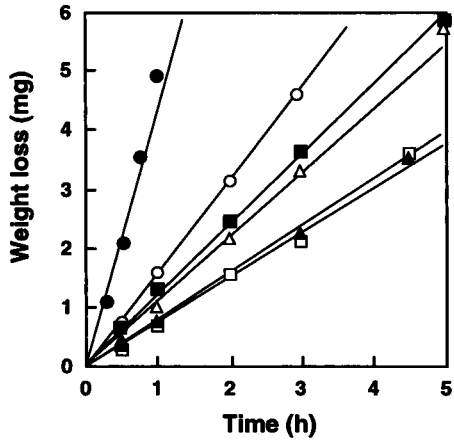

Fig. 4. Enzymatic degradation (erosion) profiles of melt-crystallized P[(*R*)-3HB-*co*-6HH] films in aqueous solution of PHB depolymerase from *A. faecalis* at 37 °C. Symbols: (●) sample 1 (Tc=30 °C), (○) sample 4 (Tc=60 °C), (■) sample 6 (Tc=70 °C), (□) sample 8 (Tc=80 °C), (▲) sample 10 (Tc=90 °C), and (△) sample 12 (Tc=100 °C).

Fig. 5 shows the scanning electron micrographs (s.e.m.) of time-dependent changes on the surfaces of P[(*R*)-3HB-*co*-6HH] film (sample 12) during the enzymatic degradation. Before enzymatic degradation, the surface of P[(*R*)-3HB-*co*-6HH] film was almost flat. After enzymatic degradation, the surface was apparently blemished with time by the action of PHB depolymerase, and the ringed texture of P[(*R*)-3HB-*co*-6HH] spherulites was detected. In addition, two different types of planes can be observed on the surface of P[(*R*)-3HB-*co*-6HH] spherulites after 0.5 h of enzymatic degradation. The smooth and rough planes exist mutually along the radial direction. The band distance of repeating two planes was determined from s.e.m., and the data are plotted in Fig. 2. The band distance of spherulites determined from the

(a) Before

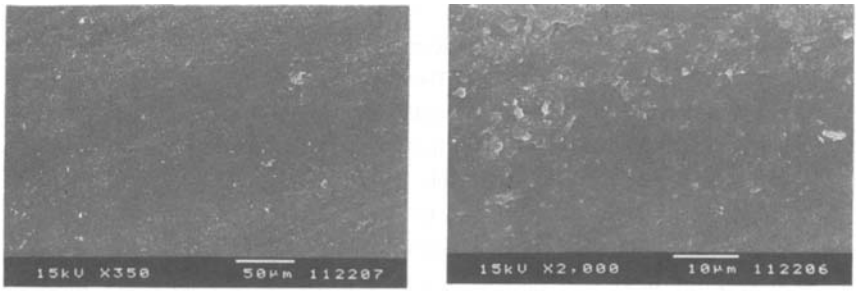

(b) After degradation for 0.5 h

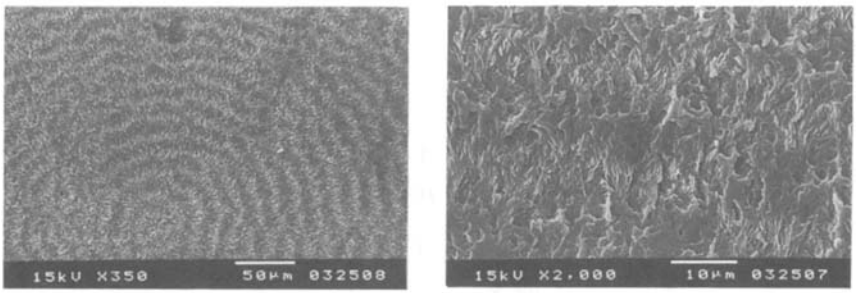

(c) After degradation for 3 h

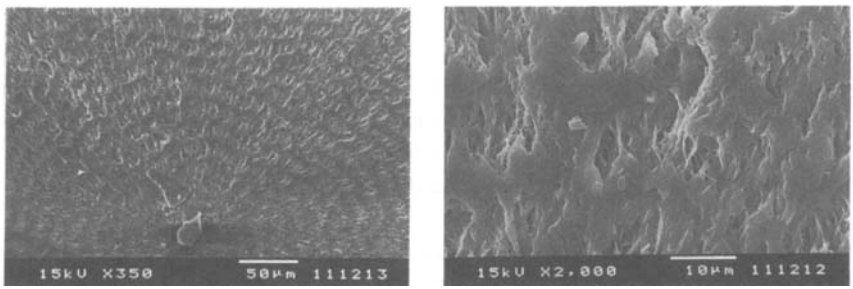

Fig. 5. Scanning electron micrographs of the surfaces of P[(*R*)-3HB-*co*-6HH] film (sample 12) before and after enzymatic degradation by PHB depolymerase from *A. faecalis*.

s.e.m. increased with an increase in the crystallization temperature for film, and the values were in good agreement with the values of band spacing determined from the optical micrographs of spherulite. The banded morphology of spherulites is well-known to arise from the difference of orientation of crystalline axis due to tuisting of lamellar crystals. Therefore, both chain-folding plane and crystal edge plane of lamellae appear on the surface of P[(*R*)-3HB-*co*-6HH] film. Hocking *et al.* (Ref. 12) and Iwata *et al.* (Ref. 13) have prepared single crystals of P[(*R*)-3HB] homopolymer and studied the enzymatic degradation of single crystals with bacterial PHB depolymerases. It has been concluded that the attack by the active site of PHB depolymerase takes place preferentially at the crystal edges rather than the chain-folding surfaces of single crystals. Also in the case of P[(*R*)-3HB-*co*-6HH] melt-crystallized film, PHB depolymerase may predominantly hydrolyze the polymer chains at the crystal edge of lamellar stacks on the film surface. Concequently, the banded morphology of P[(*R*)-3HB-*co*-6HH] spherulites was visible at the initial stage of enzymatic degradation.

REFERENCES

(1) Y. Doi, "*Microbial Polyesters*", VCH Publishers, New York 1990
(2) A. Steinbüchel, H. E. Valentin, *FEMS Microbiol. Lett.* **128**, 219 (1995)
(3) R. W. Lenz, *Adv. Polym. Sci.* **17**, 571 (1992)
(4) Y. Doi, Y. Kanesawa, N. Tanahashi, Y. Kumagai, *Polym. Degrad. Stab.* **36**, 173 (1992)
(5) T. Tanio, T. Fukui, Y. Shirakura, T. Saito, K. Tomita, T. Kaiho, S. Masamune, *Eur. J. Biochem.* **124**, 71 (1982)
(6) K. Mukai, K. Yamada, Y. Doi, *Int. J. Biol. Macromol.* **15**, 361 (1993)
(7) D. Jendrossek, A. Schirmer, H. G. Schlegel, *Appl. Microbiol.Biotechnol.* **46**, 451 (1996)
(8) H. Abe, Y. Doi, H. Aoki, T. Akehata, Y. Hori, A. Yamaguchi, *Macromolecules* **28**, 7630 (1995)
(9) Y. Kumagai, Y. Kanesawa, Y. Doi, *Makromol. Chem.* **53**, 193 (1992)
(10) G. Tomasi, M. Scandola, B. H. Briese, D. Jendrossek, *Macromolecules* **29**, 507 (1996)
(11) N. Koyama, Y. Doi, *Macromolecules* **30**, 826 (1997)
(12) P. J. Hocking, R. H. Marchessault, M. R. Timmins, R. W. Lenz, R. C. Fuller, *Macromolecules* **29**, 2472 (1996)
(13) T. Iwata, Y. Doi, K. Kasuya, Y. Inoue, *Macromolecules* **30**, 833 (1997)